J Fluoresc (2010) 20:435–440
DOI 10.1007/s10895-009-0565-9

ORIGINAL PAPER

Long Wavelength Fluorescence Lifetime Standards for Front-Face Fluorometry

Bryan J. McCranor · Richard B. Thompson

Received: 30 April 2009 / Accepted: 3 November 2009 / Published online: 2 December 2009

Abstract With the increased development and use of fluorescence lifetime-based sensors, fiber optic sensors, fluorescence lifetime imaging microscopy (FLIM), and plate and array readers, , calibration standards are essential to ensure the proper function of these devices and accurate results. For many devices that utilize a "front face excitation" geometry where the excitation is nearly coaxial with the direction of emission, scattering-based lifetime standards are problematic and fluorescent lifetime standards are necessary. As more long wavelength (red and near-infrared) fluorophores are used to avoid background autofluorescence, the lack of lifetime standards in this wavelength range has only become more apparent . We describe an approach to developing lifetime standards in any wavelength range, based on Förster resonance energy transfer (FRET). These standards are bright, highly reproducible, have a broad decrease in observed lifetime, and an emission wavelength in the red to near infrared making them well suited for the laboratory and field applications as well. This basic approach can be extended to produce lifetime standards for other wavelength regimes.

Keywords FLIM · FRET · Near infrared fluorescence · Lifetime standards · Fiber optic sensor

Introduction

Fluorescence methods are a flexible, powerful technology which can be applied to many different fields, from oceanography [1], to protein kinetics [2], to biomedicine [3–5]. Some sensors and biosensors incorporate fluorescence technology [6] to quantify analytes such as trace metals [7], amino acids [8], and many other small molecules and compounds [9–14]. Highly sensitive fluorescence methods have been adapted (for example) to fields such as neuroscience where it is used to enhance our understanding of neurodegenerative disease states like ischemic stroke [15–17]. In addition to standard fluorometers, many fluorescence methods and assays have been adapted for use in microwell plate readers, epifluorescence microscopes, and for use with array chips. An increasing number of these instruments measure fluorescence lifetimes, which have become particularly important in measurements based on Förster resonance energy transfer (FRET). The need to avoid background fluorescence and minimize attenuation in fluorescence-based fiber optic sensors and transdermal imaging has led to the development of fluorescent probes in the red to near infrared wavelengths [18–20, 34]. Although solutions of standard fluorophores are commonly used in calibration of fluorescence lifetime instrumentation in time— and frequency-domain fluorometry, [21–28], there are very few effective standards in the red to near infrared wavelength range. Simple lifetime standards such as Rayleigh scatterers are commonly used with standard fluorometers because they have a lifetime of effectively zero, allowing them to be usable with any excitation source, but these standards are generally not suitable for systems which employ (for example) fiber optics to gather information on changes in fluorescence. Unlike a standard L— or T-format fluorometer where only emission from the cuvette is directly observed and scattering from other sources is minimized by the right-angle geometry, fiber optic fluorometers have multiple optical components (objective, dichroic mirror, and the fiber optic itself) that are illuminated by the excitation in the optical path, all of which can act as sources for scattered light which is

B. J. McCranor · R. B. Thompson (✉)
Department of Biochemistry and Molecular Biology,
University of Maryland School of Medicine,
108 N. Greene Street,
Baltimore, MD 21201-1503, USA
e-mail: rthompso@umaryland.edu

collected by the detector (Fig. 1)[29]; the use of Rayleigh scatterers as standards in this type of system is infeasible because the components have differing pathlengths from the excitation source and detector, and consequently different apparent (superimposed) decays. Similar situations also occur in many microwell plate readers, array (chip) readers, and epifluorescence microscopes which also essentially have "front-face illumination" geometry where the excitation and emission beams are close to coaxial. For testing the function and alignment of these instruments, it is desirable to have fluorophore standards of known lifetimes which closely mimic the excitation and emission wavelengths of the fluorescence sensor, since the transmission of the optics and the detector response are typically wavelength-dependent. For our frequency-domain fiber optic sensor, this equates to a bright fluorophore of known phase and modulation at given modulation frequencies that can be placed at the distal end of the fiber optic, mimicking the sensor probe in Fig. 1. Moreover, since the length of fiber varies with the application, introducing a length-dependent phase shift, it is desirable to have multiple standards with differing lifetimes to provide a multipoint calibration. Similar issues obtain in lifetime-based plate readers, microscopes, and chip readers. A fluorescence lifetime standard based on Förster resonance energy transfer (FRET) [30], as described below, enables standards to be reproducibly formulated for essentially any wavelength regime with a range of lifetimes. Of course, good standards (cited above) exist for much of the ultraviolet and visible portions of the spectrum, but few exist at red and near-infrared wavelengths (the longest wavelength previously published standard we are aware of is Erythrosin B at 630 nm described in 2007 [28]), so we developed an example in the red wavelength range. In our case the standards are solutions of a fluorophore with the desired spectral characteristics mixed together with differing, specified concentrations of a colored (usually nonfluorescent) dye whose absorbance overlaps the fluorophore emission. Because of the overlap, energy transfer occurs, reducing the apparent intensity and lifetime of the donor to a degree which may be predicted by Forster's theory.

The extent of energy transfer depends on the distance between donor and acceptor molecules, benchmarked as the Förster distance (R_o) , the donor-acceptor distance where FRET is 50% efficient [30]. This implies that, for uncoupled donors and acceptors which are allowed to diffuse independently of one another, energy transfer is also dependent on the ability of the acceptor to diffuse toward the donor molecule, and vice versa, during the latter's lifetime. The extent of the transfer is thus dependent (in addition to the overlap integral, refractive index, and relative orientation) on the acceptor concentration, which for acceptors to be within typical R_0's of tens of Angstroms of the donor must be high (μM to mM) for significant energy transfer to occur [31]. When the acceptor molecules are in close proximity to the donor molecules they reduce the emission seen from the fluorophore depending on the wavelength overlap of donor emission and acceptor excitation, as well as inner filter effects. Since the acceptor molecules acquire the emission energy from the donors during the excited state, they reduce the apparent emissive lifetime of the donor in solution, so as the concentration of the acceptor is increased the lifetime of the solution emission normally decreases [30]. In phase or frequency domain fluorometry decreasing the lifetime by increasing the concentration of acceptor molecules decreases the phase

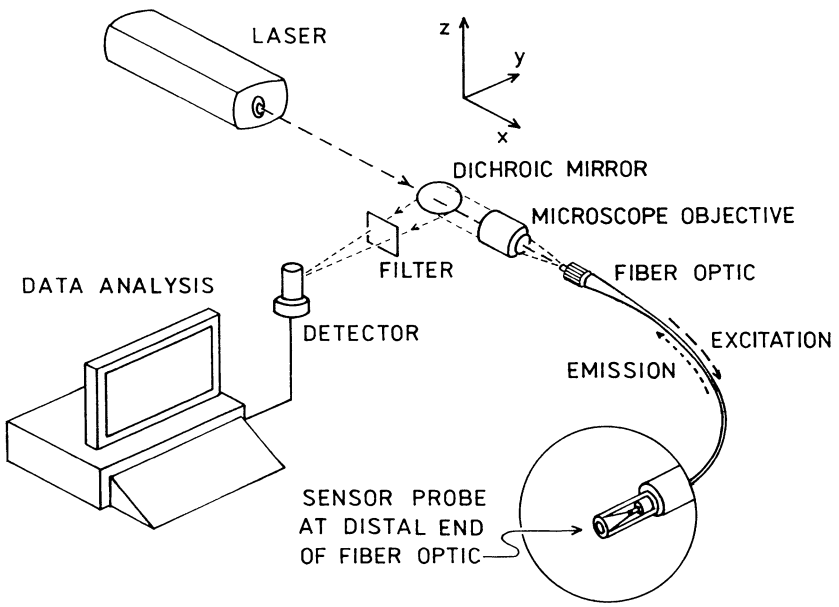

Fig. 1 Schematic of fluorescence-based fiber optic sensor. Excitation from the laser (- - -) passes through the dichroic mirror and is launched into the fiber optic at the proximal end; fluorescence (·····) comes back from the sensor at the distal end though the fiber, is collected by the microscope objective, is reflected off the dichroic mirror, and passes through the emission filter to be collected by the detector. Reproduced from [29] with permission

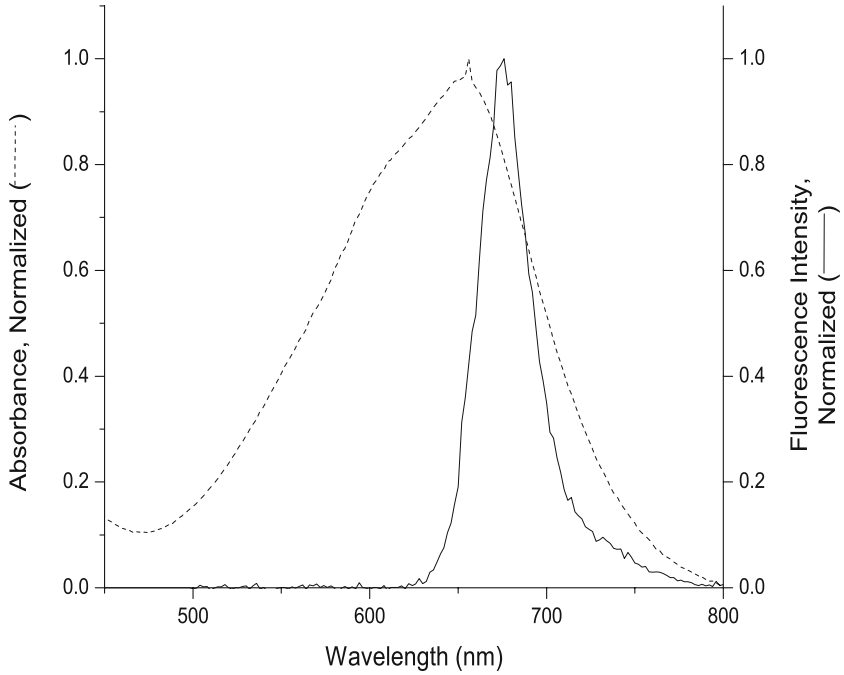

Fig. 2 Spectral overlap of the emission spectrum of DTDCI in ethanol (solid line) with the absorption spectrum of Janus Green B in ethanol (dashed line)

angle of the emission and increases the modulation ratio, at all modulation frequencies. In order to properly fit the frequency-dependent phase and modulation curves one would normally have to account for the diffusion of the donor and acceptor molecules when in solution [32]. In this study, though, the fluorophore chosen, Diethylthiadicarbocyanine Iodide (DTDCI) has a known short lifetime of 1.7*ns* [33], so that in ethanol, at room temperature, donor and acceptor can only diffuse a short distance during the donor lifetime. The diffusion coefficients for donor (DTDCI) and acceptor (Janus Green B) molecules under these conditions were calculated from estimated bond lengths of the compounds. The coefficients were 3.36×10^{-10} $m^2\bullet s^{-1}$, and 1.55×10^{-10} $m^2\bullet s^{-1}$ in ethanol at 25°C respectively, which correlate to a diffusion distance, in ethanol, of 10.69 Å for DTDCI and 7.27 Å for Janus Green B during the lifetime of DTDCI (1.7*ns*) . Both of these distances are well below the calculated Förster distance for the pair, R_o=49.7 Å. Also, the lowest concentration of Janus Green B in use here is more than 16-fold higher than the concentration that would place an acceptor on the average at a distance equal to R_0 [31]. The effect of diffusion on the donor decay is then very small, and the frequency-dependent phase and modulation data generated in the study are for the most part well fit by a monoexponential model, as shown by Lakowicz, et al. [32]. If the donor had a much longer lifetime; and/or the donor-acceptor pair had a poorer overlap; and/or the pair could diffuse much faster due to small size, low viscosity, and/or high temperature; diffusion would become important and the time dependent decay would be non-exponential. We note that it is convenient but not necessary that the decay be monoexponential; for our purposes the frequency-dependent phase and modulation need only be reproducible, which is straightforward since at a particular temperature they are mainly functions of the acceptor concentration. Fortunately, for a given wavelength regime it is usually possible to identify a donor-acceptor pair with excellent overlap and a relatively short donor lifetime such that solutions exhibiting a range of lifetimes can be readily formulated.

Table 1 Lifetimes of DTDCI/Janus green B mixtures from single and two component fits

Janus Green B (μM)	Single component τ (ns)	Single component χ2	Two component τ_1 (ns)	f_1	Two component τ_2 (ns)	f_2	χ2
0	1.67±0.004	33.6	1.7±0.005	1.01	$2.24\times10^6\pm0$	263	30.3
32.5	1.47±0.004	31.2	1.59±0.02	0.898	0.451±0.09	0.095	15.2
97.5	1.21±0.003	83.2	0.754±0.02	0.508	1.89±0.06	0.485	21.6
162.5	0.968±0.003	175	0.445±0.01	0.487	1.75±0.03	0.515	8.37

Standard errors of 0.30 and 0.003 where used for the fits of phase delay and modulation ratio to calculate χ^2 respectively. The modulation ratio for 97.5μM Janus Green B was scaled by a factor of 1.02 while the modulation ratio for 162.5μM Janus Green B was scaled by a factor of 1.05

Experimental

Materials

Ethanol and fluorophores used were of the highest purity commercially available and were not purified further. Rose Bengal and Janus Green B (65% Dye) were obtained from Sigma-Aldrich; Diethylthiadicarbocyanine Iodide was originally obtained from Eastman Organics Company, Rochester, NY.

Instrumentation

Multifrequency phase fluorometric measurements were performed on an ISS K2 (ISS Inc., Champaign, IL) fluorometer. Excitation at 514*nm* was provided by a Spectra Physics Argon Ion laser (Model # 2065) (Newport Corp., Spectra-Physics Div., Mountain View, CA) for experiments in cuvettes. Emission was measured through an RG595 filter and Glan-Thompson polarizers in "magic angle" configuration. Frequency-dependent phase and modulation data were collected and analyzed by ISS Vinci software (ISS Inc., Champaign, IL).

Method

DTDCI was chosen as the donor molecule, due to its emission in the red/near infrared (NIR), similar to existing fiber optic Cu(II) sensors, and its known short lifetime [33]. Janus Green B was chosen as the acceptor molecule, due to near-perfect overlap of its absorbance spectrum with the emission spectrum of DTDCI (Fig. 2). Increasing concentrations of Janus Green B were added to 10μM DTDCI in ethanol to give a range of solutions with 0 – 162.5 μM of acceptor molecules. A solution of Rose Bengal in ethanol was used as a reference because of its accepted lifetime of 0.752*ns* [25] . Neutral density filters were placed in the pathway of the excitation and Rose Bengal emission light, and a RG595 filter was placed in the pathway of the sample emission light to eliminate artifacts due to scattered light. Master and slave synthesizers were set to 6.0 *dBm* and 3.*0 dBm* respectively. The excitation wavelength was set to 514*nm* and measurements were carried out in 0.7*ml* cuvettes due to inner filter effects, this closely mimics a fiber optic sensor since 655*nm* excitation only penetrates a short distance at these concentrations of Janus Green B. Emission data were recorded using the ISS Vinci software, and frequency-dependent phase and modulation data and lifetime data were analyzed using both mono-exponential and two exponential models. During data analysis the phase delay standard error was set to 0.3 degrees and the modulation ratio standard error to 0.003, the modulation ratios for the two highest Janus Green B concentrations (97.5μM and 162.5μM) were multiplied by factors of 1.02 and 1.05 to correct a modulation artifact.

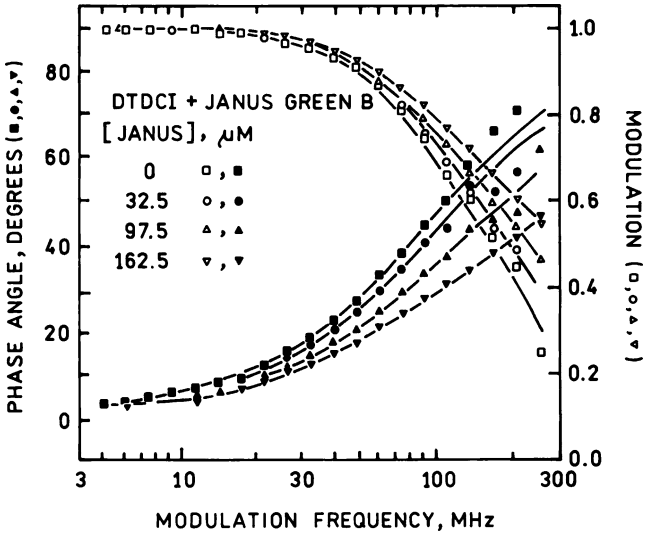

Fig. 3 Frequency-dependent phase and modulation data of the lifetime standards; DTDCI (■), together with 32.5μM (●), 97.5μM (▲), and 162.5μM (▼) Janus Green B. Open symbols represent the modulation ratio, closed symbols represent the phase delay, lines indicate the best single component fits to the data (except for 97.5μM and 162.5μM Janus Green B where two component fits were used). It should be noted that the modulation ratios for 97.5μM and 162.5μM were scaled by factors of 1.02 and 1.05 respectively

Table 2 Lifetimes of DTDCI/Janus green B mixtures from phase only fits

Janus Green B (μM)	Phase only τ (ns)	Phase only χ^2
0	1.78	30.7
32.5	1.42	38.4
97.5	1.10	71.4
162.5	0.811	105

A standard error of 0.03 was used for the phase fits

Table 3 DTDCI/Janus green B phase and modulation data at 109*MHz*

Janus Green B (μM)	Phase Angle	Modulation Ratio
0	49.97	0.6727
32.5	43.42	0.6871
97.5	36.82	0.7311
162.5	30.72	0.7685

Data was generated by green excitation. The modulation ratios for 97.5μM and 162.5μM were scaled by factors of 1.02 and 1.05 respectively

Results and discussion

As expected, increasing the concentration of Janus Green B decreased the apparent donor emission lifetime (Table 1). While we expected the lifetime data generated to be well fit to a monoexponential decay, the frequency-dependent phase and modulation data for the higher Janus concentrations ($97.5\mu M$ and $162.5\mu M$ Janus) were better fit to two lifetime components, as is seen in the decrease in χ^2. This difference in best fits, between lower concentrations of Janus Green B and higher, may be due to a modulation artifact in the DC current. Evidence for such an artifact is seen in the modulation data, which plateau at low frequencies slightly below 100% and in fits to phase only generated data, which report similar lifetimes to the corrected phase and modulation data (Table 2). The significantly better fits to two components at the highest concentrations of Janus Green B could also be attributed to some sort of weak complex or the presence of impurities; commercially available Janus Green B assays only 65% due to the presence of salt used in its preparation. When the data are fit, the derived phase and modulation values from the model differ only slightly from the measured data, which can be seen on the frequency-dependent phase and modulation plot (Fig. 3).

For convenience, calibration of fiber optic instrumentation can be accomplished by measuring the phase delay and modulation ratio at one modulation frequency of multiple standard mixtures, which can be done rapidly. The decrease in phase angle and increase in modulation ratio of samples of increasing acceptor molecule concentration is clearly shown by data taken at a frequency of $109MHz$ (Table 3). The highest concentration of Janus Green B ($162.5\ \mu M$) causes the measured phase angle to decrease 19.25^{o} at $109MHz$ from the phase of DTDCI alone, while the modulation ratio increases 9.58%. Use of long multimode fiber optics with sensors at the distal end creates a length-dependent phase delay and demodulation due to modal dispersion in the fiber; both these effects can be corrected for by measuring the known phases and modulations of three or four standard solutions at the distal end of the fiber.

Conclusion

As fluorescence technology becomes more advanced and flexible in its applications, its use outside the research laboratory will become more prevalent [1], as will fluorescent probes that push the boundaries into the red and near infrared wavelengths [5, 34–36]. Since their introduction in the Eighties, a variety of fluorescence lifetime-based sensors have devised for numerous purposes. Among the most important current uses of lifetime measurements is to measure FRET, as it has emerged that intensity-based methods of measuring FRET (particularly between GFP variants with substantial spectral bleed-through) are easier but require substantial correction that compromises accuracy ; by comparison, lifetime measurements are more “rigorous” and “unambiguous” [37]. As FLIM instrumentation (now commercially available) becomes more widespread, one can expect its use to measure FRET will be correspondingly greater [38–40]. The increasing use of long wavelength fluorophores is due not only to the reduced background fluorescence, but to reduced scattering and absorbance, particularly in living tissue; hence there has been substantial interest in long wavelength fluorophores for use in transdermal imaging and sensing[18, 41]. For such imaging applications even longer wavelength standards (c. 800 nm) will be needed than those described here, but our same approach may be used with a suitable FRET pair in that wavelength range. We note that for lifetime imaging applications such as microscopy, plate reading, or transdermal imaging *in vivo,* the time response of the system typically varies across the visual field, and correction using lifetime standards is essential [42, 43]. In all these cases, more flexible calibration standards must be created to ensure proper function of fiber optic fluorescence sensors, FLIM microscopes, and array and plate readers. We report the development of such a set of standards, based on the FRET pair of DTDCI and Janus Green B. These bright and readily reproducible standards report a broad decrease in phase angle and increase in modulation ratio, which correlate to an overall decrease in lifetime. Due to the short lifetime of DTDCI, $1.7ns$ [33] , a simple mono-exponential fit can be applied to the frequency-dependent phase an modulation data, as previous investigators have shown when using a fluorophore with a short lifetime ($\sim 1\ ns$) that the fluorescent event will occur in such a time period in which diffusion does not need to be accounted for [32]. The generality of this approach makes it appealing for the development of standards at longer wavelengths especially.

Acknowledgements We would like to thank the NIH (grant R01 EB003924) for support and Henryk Szmacinski for all of his helpful discussions.

References

1. Zeng HH, Thompson RB, Maliwal BP, Fones GR, Moffett JW, Fierke CA (2003) Real-time determination of picomolar free cu(ii) in seawater using a fluorescence-based fiber optic biosensor. Anal Chem 75(24):6807–6812
2. Lin C-H, Chen H-Y, Yi C-J, Lu P-L, Hsieh C-H, Hsieh B-Y, Chang Y-F, Chou C (2009) Quantitative measurement of binding kinetics in sandwich assay using a fluorescence detection fiber-optic biosensor. Anal Biochem 385:224–228

3. Peterson JI, Goldstein SR, Fitzgerald RV, Buckhold DK (1980) Fiber optic ph probe for physiological use. Anal Chem 52:864–869
4. Cullum BM, Vo-Dinh T (2000) The development of optical nanosensors for biological measurements. Trends biotechnol 18:388–393
5. Bozym RA, Thompson RB, Stoddard AK, Fierke CA (2006) Measuring picomolar intracellular exchangeable zinc in pc-12 cells using a ratiometric fluorescence biosensor. ACS Chemical Biology 1(2):103–111
6. Fierke CA, Thompson RB (2001) Fluorescence-based biosensing of zinc using carbonic anhydrase. Biometals 14:205–222
7. Thompson RB, Maliwal BP, Fierke CA (1999) Selectivity and sensitivity of fluorescence lifetime-based metal ion biosensing using a carbonic anhydrase transducer. Anal Biochem 267:185–195
8. Lam H, Kostov Y, Rao G, Tolosa L (2008) Low-cost optial lifetime assisted ratiometric glutamine sensor based on glutamine binding protein. Anal Biochem 383:61–67
9. Mohr GJ, Wolfbeis OS (1995) Optical sensing of anions via polarity-sensitive dyes: A bulk sensor membrane for nitrate. Anal Chim Acta 316:239–246
10. Stevenson CL, Vo-Dinh T (1995) Analysis of polynuclear aromatic compounds using laser-excited synchronous fluorescence. Anal Chim Acta 303:247–253
11. Li Y-S, Lui W-P, Gao X-F, Chen D-D, Li W-G (2008) Immobilized enzymatic fluorescence capillary biosensor for determination of sulfated bile acid in urine. Biosens Bioelectron 24:538–544
12. Schrenkhammer P, Wolfbeis OS (2008) Fully reversible optical biosensors for uric acid using oxygen transduction. Biosens Bioelectron 24:994–999
13. Salonikidis PS, Zeug A, Kobe F, Ponimaskin E, Richter DW (2008) Quantitative measurement of camp concentration using an exchange protein directly activated by a camp-based fret-sensor. Biophys J 95:5412–5423
14. Salinas-Castillo A, Pastor I, Mallavia R, Mateo CR (2008) Immobilization of a trienzymatic system in a sol-gel matrix: A new fluorescent biosensor for xanthine. Biosens Bioelectron 24:1053–1056
15. Wei G, Hough CJ, Li Y, Sarvey JM (2004) Characterization of extracellular accumulation of zn2+ during ischemia and reperfusion of hippocampus slices in rat. Neuroscience 125:867–877
16. Zeng H-H, Bozym RA, Rosenthal RE, Fiskum G, Cotto-Cumba C, Westerberg N, Fierke CA, Stoddard A, Cramer ML, Frederickson CJ, Thompson RB (2005) *In situ measurement of free zinc in an ischemia model and cell culture using a ratiometric fluorescence-based biosensor*. in *SPIE Conference on Advanced Biomedical and CLinical Diagnostic Systems III*. SPIE, San Jose
17. Stork CJ, Li YV (2006) Intracellular zinc elevation measured with a "calcium-specific" indicator during ischemia and reperfusion in rat hippocampus: A question on calcium overload. J Neurosci 26 (41):10430–10437
18. B. Chance,R. R. Alfano,B. J. Tromberg,M. Tamura,andE. M. Sevick-Muraca, eds. *Optical tomography and spectroscopy of tissue vi*. 2005, Society of Photooptical Instrumentation Engineers. 550 pp
19. Teles FRR, Fonseca LP (2008) Trends in DNA biosensors. Talanta 77:606–623
20. Goncalves HMR, Maule CD, Jorge PAS, Silva J C G E d (2008) Fiber optic lifetime ph sensing based on ruthenium(ii) complexes with dicarboxybipyridine. Anal Chim Acta 626:62–70
21. Chen RF (1974) Fluorescence lifetime reference standards for the range of 0.189 to 115 nanoseconds. Anal Biochem 57:593–604
22. Barrow DA, Lentz BR (1983) The use of isochronal reference standards in phase and modulation fluorescence lifetime measuremens. J Biochem Biophys Methods 7:217–234
23. Lampert RA, Chewter LA, Phillips D, O'Connor DV, Roberts AJ, Meech SR (1983) Standards for nanosecond fluorescence decay time measurements. Anal Chem 55:68–73
24. Gratton E, Limkeman M, Lakowicz JR, Maliwal BP, Cherek H, Laczko G (1984) Resolution of mixtures of fluorophores using variable-frequency phase and modulation data. Biophys J 46:479–486
25. Lakowicz JR, Laczko G, Gryczynski I (1986) 2-ghz frequency-domain fluorometer. Rev Sci Instrum 57(10):2499
26. Thompson RB, Gratton E (1988) Phase fluorimetric measurement for determination of standard lifetimes. Anal Chem 60:670–674
27. Lakowicz JR, Gryczynski I, Laczko G, Gloyna D (1991) Picosecond fluorescence lifetime standards for frequency- and time-domain fluorescence. J. fluoresc 1(2):87
28. Boens N, Qin W, Basaric N, Hofkens J, Ameloot M, Pouget J, Lefevre J-P, Valeur B, Gratton E, Ven M V d, Silva ND, Engelborghs Y, Katrien W, Sillen A, Rumbles G, Phillips D, Visser AJWG, Hoek A v, Lakowicz JR, Malak H, Gryczynski I, Szabo AG, Krajcarski DT, Naoto T, Atsushi M (2007) Fluorescence lifetime standards for time and frequency domain fluorescence spectroscopy. Anal Chem 79(5):2137–2149
29. Thompson RB, Hui-Hui Zeng, Ohnemus D, McCranor B, Cramer M, Moffett J (2008) In: Brand L, Johnson ML (eds) Fluorescence spectroscopy. Academic, San Diego, pp 311–337
30. Forster T (1948) Intermolecular energy migration and fluorescence (ger.). Annalen der Physik 2:55–75
31. Lakowicz JR (1999) *Principles of fluorescence spectroscopy* in Second ed. Kluwer Academic / Plenum Publishers, New York
32. Lakowicz JR, Szmacinski H, Gryczynski I, Wiczk W, Johnson ML (1990) Influence of diffusion on excitation energy transfer in solutions by gigahertz harmonic content frequency-domain fluorometry. J Phys Chem 94:8413–8416
33. Thompson RB, Frisoli JK, Lakowicz JR (1992) Phase fluorometry using a continuously modulated laser diode. Anal Chem 64:2075–2078
34. Thompson RB (1994) Topics in fluorescence spectroscopy vol. 4. In: Lakowicz JR (ed) Probe design and chemical sensing. Plenum Press, New York, pp 151–181
35. Lakowicz JR, Piszczek G, Kang JS (2001) On the possibility of long-wavelength long-lifetime high-quantum-yield luminophores. Anal Biochem 288:62–75
36. Campbell RE, Tour O, Palmer AE, Steinbach PA, Baird GS, Zacharias DA, Tsien RY (2002) A monomeric red fluorescent protein, *Proceedings of the National*. Academy of Sciences 99 (12):7877–7882
37. Piston DW, Kremers G-J (2007) Fluorescent protein fret: The good, the bad, and the ugly. Trends Biochem. Sci 32(9):407–413
38. Bacskai BJ, Skoch J, Hickey GA, Allen R, Hyman BT (2003) Fluorescence resonance energy transfer determinations using fluorescence lifetime imaging microscopy to characterize amyloid plaques. J. Biomed. Opt 8(3):368–375
39. Domingo B, Sabariegos R, Picazo F, Llopis J (2007) Imaging fret standards by steady-state fluorescence and lifetime methods. Microsc Res Tech 70:1010–1021
40. Thompson RB (2008) Optical biosensors. In: Ligler FS, Taitt CR (eds) Today and tomorrow. Elsevier, Amsterdam, pp 287–315
41. Fisher G, Ballou B, Srivastava M, Farkas DL (1996) Far-red fluorescence-based high specificity tumor imaging in vivo. Biophys J 70(2):212A
42. Lakowicz JR, Szmacinski H, Nowaczyk K, Berndt K, Johnson ML (1992) Fluorescence lifetime imaging. Anal Biochem 202:316–330
43. H. Szmacinski,J. R. Lakowicz and M. L. Johnson (1994) in M. L. Johnson and L. Brand (Ed.), *Numerical computer methods*, Academic Press, New York, pp. 723–748